Band structures and characteristics of InGaAs/ InGaAsP strain-compensated quantum well lasers

C.S. MA[1], L.J. WANG[2] AND S.Y. LIU[1]

[1]*Department of Electronic Engineering, State Key Laboratory on Integrated Optoelectronics, Jilin University, Changchun 130023, China;*
[2]*Laboratory of Excited State Processes, Changchun Institute of Optics, Fine Mechanics and Physics, Chinese Academy of Sciences, Changchun 130021, China*

Abstract. Analysis is performed for valence band structures and some characteristics of InGaAs/InGaAsP strain-compensated quantum well lasers lattice-matched to InP substrate. The computed results show that band offsets are functions of strain compensation instead of constants; strain compensation changes the band structures and the density of states, and hence affects the optical gain and the threshold current density. Under the condition of zero net strain, the values of the well width, cavity length and relative threshold carrier density and threshold current density are determined for realization of 1.55 μm wavelength emission.

1. Introduction

In recent years considerable attention and great efforts have been focused on the development of strain-compensated quantum well (SCQW) materials (Streubel *et al.* 1976; Tu *et al.* 1995; Silfvenious *et al.* 1997) and devices, such as diode lasers (Miller *et al.* 1991; Zhang and Ovtchinnikov 1993; Chua *et al.* 1994; Lin *et al.* 1994; Hillmer *et al.* 1995; Kasukawa *et al.* 1995a, b; Park *et al.* 1995), electroabsorption modulators (Ougazzaden *et al.* 1997) and optical amplifiers (Ougazzaden *et al.* 1995), because of their excellent features and wide applications in optical communication systems, particularly in optical signal and data processing.

Strain compensation modifies the band structures of SCQW systems more agilely, leads to the increase of the critical thickness without defect generation in the material. This can prevent the features of the device going bad and maintain the operation of device much better (Miller *et al.* 1991; Hillmer *et al.* 1995; Kasukawa *et al.* 1995a, b; Park *et al.* 1995).

Band offsets between the well and the barrier in SCQW structures are very important parameters, which strongly affect the band structures of SCQW devices. In the usual case, band offsets in a SCQW system are functions of

material compositions and hence strain compensation instead of constants as assumed in some previous investigations (Park *et al.* 1995). Analysis of the band structure is the basis of studying some other important properties of SCQW devices, such as the density of states, optical gain, injection carrier density and threshold current density.

In this paper, the following InGaAs/ InGaAsP SCQW laser configuration is adopted in our calculation. The layers in this configuration are in turn: InP substrate, InGaAsP unstrained confined layer (lattice-matched to InP, 1.1 μm bandgap), InGaAsP strained barrier, InGaAs strained well, InGaAsP strained barrier, InGaAsP unstrained confined layer (lattice-matched to InP, 1.1 μm bandgap), and InP capping layer. So the lattice constant of every layer is equal to that of InP. In our calculation, the material interpolation principle presented in Nido *et al.* (1993) is used to determine the values of material parameters of InGaAs and InGaAsP by using those of InAs, GaAs and InP which are taken from Nido *et al.* (1993) and Ishikawa and Bowers (1994). Also, analysis is carried out for the band offsets, valence band structure, density of states, optical gain and threshold current density of this laser configuration. Furthermore, in order to realize 1.55 μm wavelength emission of this laser configuration with zero net strain, the values of the well width, cavity length and relative threshold carrier density and threshold current density are determined. Finally based on the analysis and the discussion, some conclusions are summarized.

2. Strains in the well and the barrier

The strains in the InGaAs well ε_1 and in the InGaAsP barrier ε_2 are defined as

$$\varepsilon_1 = (a_1 - a)/a_1, \quad \varepsilon_2 = (a_2 - a)/a_2, \tag{1}$$

where a_1 and a_2 are untrained lattice constants of the well and the barrier, respectively, $a_1 = a(\text{InGaAs})$ and $a_2 = a(\text{InGaAsP})$, and a is the strained lattice constant of the total SCQW structure when strains exist in the well and the barrier, which is equal to that of InP, $a = a(\text{InP})$.

Fig. 1 shows the relation between the indium and arsenic compositions x, y and the strain ε_2 in the $\text{In}_x\text{Ga}_{1-x}\text{As}_y\text{P}_{1-y}$ barrier, and the top frame ($y = 1$) corresponds to the relation between the indium composition x and the strain ε_1 in the $\text{In}_x\text{Ga}_{1-x}\text{As}$ well. We find that the values of the compositions of indium and arsenic x and y in the InGaAsP barrier can result in either tensile ($\varepsilon_2 < 0$) or compressive ($\varepsilon_2 > 0$) strain in the barrier depending on whether $x + 0.47y - 1 < 0$ or $x + 0.47y - 1 > 0$. When $x + 0.47y - 1 = 0$, the lattice constant of the InGaAsP barrier is matched to that of InP ($\varepsilon_2 = 0$). We can also find that the value of the indium composition x in the InGaAs well
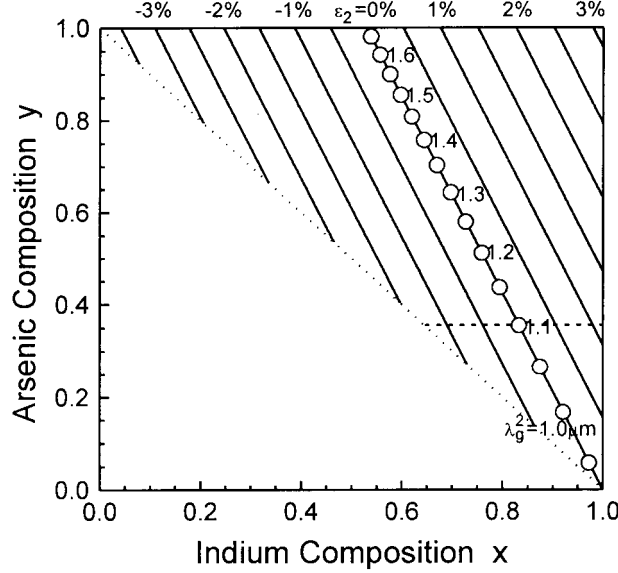
Fig. 1. Constant strain lines in the xy-plane for $In_xGa_{1-x}As_yP_{1-y}$ barrier, in which $y = 1$ corresponds to $In_xGa_{1-x}As$ well.

can also lead to either tensile ($\varepsilon_1 < 0$) or compressive ($\varepsilon_1 > 0$) strain in the well depending on whether $x < 0.53$ or $x > 0.53$. When $x = 0.53$, the lattice constant of the InGaAs well is also matched to that of InP ($\varepsilon_1 = 0$). In the following calculations the values of the indium and arsenic compositions x and y in the InGaAsP barrier are selected along the dashed straight line as shown in Fig. 1. This dashed straight line parallels to the x-axis and passes through the point ($x = 0.833$ and $y = 0.355$) of 1.1 μm barrier bandgap lattice-matched to InP, that is, we keep the value of $y = 0.355$ as a constant when the value of x is changed.

3. Band offsets between the well and the barrier

When strains exist in the well and the barrier, the band offsets of the conduction band for the electron and the valence band for the heavy- and light-holes ΔE_c, ΔE_{hh} and ΔE_{lh} between the well and the barrier can be expressed as

$$\Delta E_c = (E_{g0}^2 - E_{g0}^1) + (\Delta E_0^2 - \Delta E_0^1) + (V_c^2 - V_c^1),$$
$$\Delta E_{hh} = (\Delta E_0^1 - \Delta E_0^2) - (V_{hh}^1 - V_{hh}^2), \tag{2}$$
$$\Delta E_{lh} = (\Delta E_0^1 - \Delta E_0^2) - (V_{lh}^1 - V_{lh}^2),$$

respectively, where E_{g0}^j is the unstrained bandgap of the well and the barrier, ΔE_0^j are the unstrained valence-band edge energies of the well and the barrier

from InP valence-band edge, V_{c}^{j}, V_{hh}^{j} and V_{lh}^{j} are the strained potentials of the conduction band for the electron and the valence band for the heavy- and light-holes, of which the expressions are given in Hong et al. (1987).

Fig. 2 shows the dependence of the band offsets of the conduction band for the electron and the valence band for the heavy- and light-holes ΔE_{c}, ΔE_{hh} and ΔE_{lh} on the strain compensation between the InGaAs well and the InGaAsP barrier, where the strain ε_{2} in the barrier is opposite to the strain ε_{1} in the well. As the strain ε_{1} in the well increases from the negative (tensile) to the positive (compressive), the band offsets ΔE_{c} and ΔE_{hh} increase, while ΔE_{lh} decreases. On the contrary, as the strain ε_{2} in the barrier increases from the negative (tensile) to the positive (compressive), the band offsets ΔE_{c} and ΔE_{hh} decrease, while ΔE_{lh} increases. In the case that the strain ε_{1} in the well is negative (tensile) and the strain ε_{2} in the barrier is positive (compressive), the conduction band offset for the electron ΔE_{c} may be reduced to zero or negative. Thus the original electron well will be turned into electron barrier, and the SCQW system is transformed from type I into type II. In order to keep the SCQW system as type I, the band offset ΔE_{c} should be positive, such strain compensation should be selected, in which the strain in the well is positive and that in the barrier is negative, that is, $\varepsilon_{1} > 0$ and $\varepsilon_{2} < 0$. In our calculation we choose the compressive strain in the well as a typical value $\varepsilon_{1} = 1.5\%$, and take the tensile strain in the barrier within the range of $-1.0\% \leq \varepsilon_{2} \leq 0\%$. The widths of the well and the barrier are $b_{1} = 3.4$ nm and $b_{2} = 6.8$ nm,
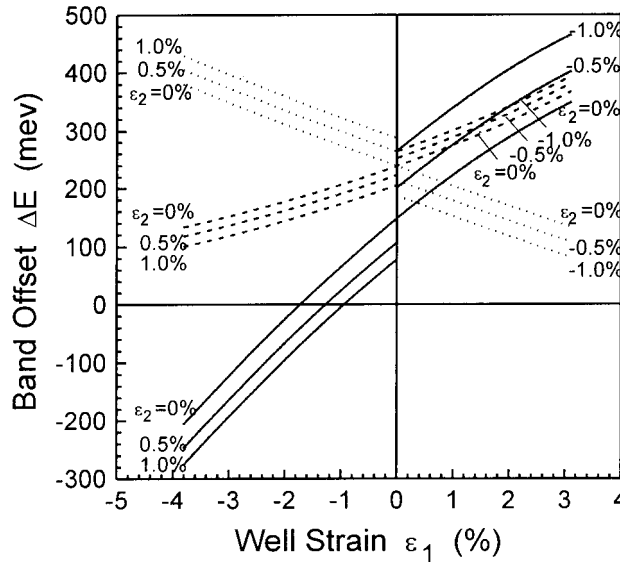

Fig. 2. Band offsets of conduction band for electron and valence band for heavy- and light-holes ΔE_{c} (solid line), ΔE_{hh} (dashed line) and ΔE_{lh} (dotted line), where the values of the indium and arsenic compositions x and y are selected along the dashed straight line in Fig. 1.

respectively. Under the condition of the above parameters, the emission wavelength of the SCQW laser is within the range of 1.5 to 1.6 μm.

4. Valence band structure

4.1. ENERGY LEVELS AT THE Γ POINT

At the Γ point because the full band mixing effect does not exist between the valence subbands, the Kohn–Luttinger Hamiltonian (KLH) (Hong *et al.* 1987) is reduced to the Schrödinger equation. We can solve the Schrödinger equation to obtain the values of the top energies of the valence subbands at the Γ point. Fig. 3 shows the effect of the tensile strain ε_2 in the barrier on the top energies E_z of the valence subbands at the Γ point. The energy levels E_z at the Γ point of the subbands HH1, HH2 and LH1 are in the well (between the valence band edges of the InGaAs strained well and InGaAsP strained barrier), while those of the subbands LH2 and LH3 are out of the well (between the valence band edges of the InGaAsP strained barrier and the InGaAsP unstrained confined layer lattice-matched to InP). The values of E_z decreases slightly for the heavy-subbands HH1 and HH2 but increases for the light-subbands LH1, LH2 and LH3 with an increase in the tensile strain ε_2 in the barrier (meaning its absolute value and the same below). This is because as the tensile strain in the barrier increases, the depth of the well for the heavy-hole becomes deeper while that for the light-hole becomes shallower.
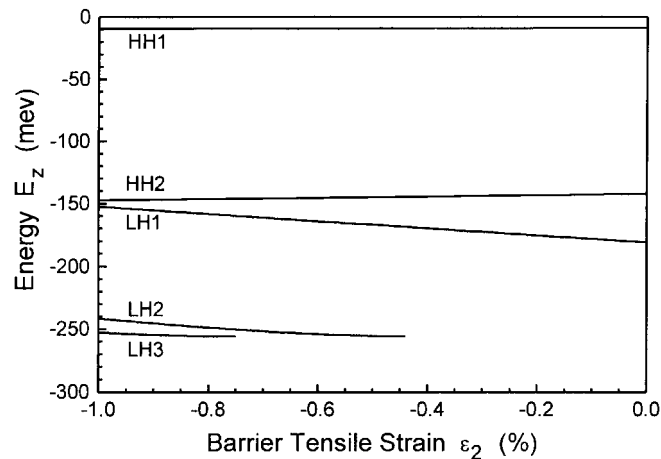

Fig. 3. Energy levels E_z at the tops of valence subbands HH1, HH2, LH1, LH2 and LH3 versus tensile strain ε_2 in the barrier, where the well width $b_1 = 3.4$ nm, the barrier width $b_2 = 6.8$ nm, and the compressive strain in the well $\varepsilon_1 = 1.5\%$.

4.2. ENERGY SUBBANDS AT THE NON-Γ POINTS

At the non-Γ points because the full band mixing effect exists between the valence subbands, we must solve the KLH equation to obtain the values of the valence band energy, of which the expression is chosen for Hong *et al.* (1987). In the calculation the energy representation technique presented in Ma *et al.* (1997) is used to solve the KLH equation, in which the order of the energy characteristic matrix equals twice the number of the energy levels at the Γ point. Fig. 4 shows the effect of the tensile strain ε_2 in the barrier on the valence energy, and only the curves of the HH1, HH2 and LH1 subbands are plotted, where we take the tensile strain in the barrier as $\varepsilon_2 = 0$, −0.5 and −1.0%, respectively. It is found that strain compensation makes the light-hole subband LH1 rises up obviously. It is also found that strain compensation makes the heavy-hole subbands HH1 and HH2 go down slightly when they are near the tops, but makes them rise up evidently when they are far from the tops.

4.3. CONSTANT ENERGY LINES OF THE VALENCE SUBBANDS

We can find from Fig. 4 that the energy curves of the valence subbands have different shapes along different directions of the wavevector $\vec{k}_\parallel$. Here we only plot the constant energy line distribution of the HH1 first subband in Fig. 5, where we take the tensile strain in the barrier as $\varepsilon_2 = 0$, −0.5 and −1.0%, and the energy values as $E_v = -50$, −100, −150, −200 and −250 mev, respectively.
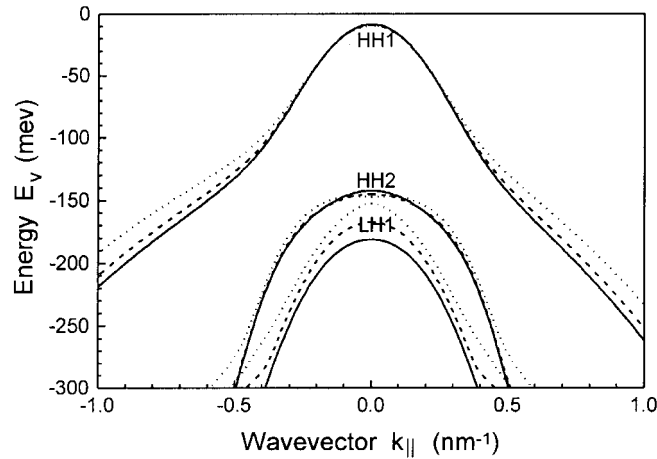

Fig. 4. Valence subbands HH1, HH2 and LH1 versus wavevector $k_\parallel$, where the well width $b_1 = 3.4$ nm, the barrier width $b_2 = 6.8$ nm, the compressive strain in the well $\varepsilon_1 = 1.5\%$, and the tensile strain in the barrier $\varepsilon_2 = 0\%$ (solid lines), −0.5% (dashed lines) and −1.0% (dotted lines).
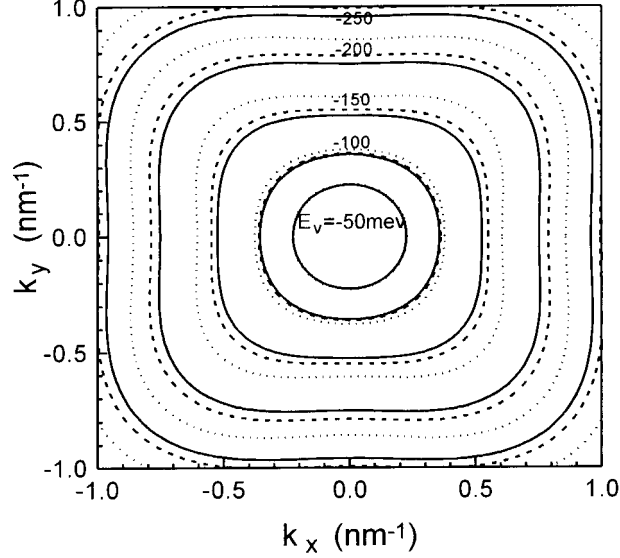
Fig. 5. Constant energy lines of HH1 first subband in Fig. 4, where the well width $b_1 = 3.4$ nm, the barrier width $b_2 = 6.8$ nm, the energy $E_v = -50$, -100, -150, -200 and -250 mev, the compressive strain in the well $\varepsilon_1 = 1.5\%$, and the tensile strain in the barrier $\varepsilon_2 = 0\%$ (solid lines), -0.5% (dashed lines) and -1.0% (dotted lines).

It can be seen that near the top of the HH1 subband, the constant energy lines are nearly circular. This shows that the energy has identical values along all the directions of the wavevector $\vec{k}_\parallel$. When the energy is far from the top, the constant energy lines are no longer circular, so the energy has different values along different directions of the wavevector $\vec{k}_\parallel$. This indicates that only for the case of energy near the top of the subband, we can make the constant energy approximation of the valence subbands of the heavy- and light-holes along all the directions of the wavevector $\vec{k}_\parallel$.

4.4. CARRIER CONTRIBUTIONS ON THE VALENCE SUBBANDS

The charge neutrality condition is assumed in the following calculations, that is, the density of the electrons in the conduction band n equals that of the holes in the valence band p, so the carrier density $N = n = p$. Fig. 6(a) shows the percentages of the carrier density N_i/N for the valence subbands HH1, HH2 and LH1, where we take the tensile strain in the barrier as $\varepsilon_2 = -0.5\%$. We can find that more than 90% of the carriers are contributed on the HH1 first subband when the total carrier density N is less than 10^{19} cm^{-3}. This indicates that the carrier transition mainly occurs between the first pair of subbands in the conduction band and the valence band, therefore, this carrier transition plays a very important role in the improvement of the features of

the laser. The percentage of the carrier density N_1/N of the HH1 first sub-band is nearly kept a constant when the total carrier density N is less than 10^{18} cm^{-3}, but it decreases evidently when the total carrier density N is larger than 10^{18} cm^{-3}. In the following discussion of Fig. 12 we will find that the threshold carrier density of a SCQW laser is in the order of 10^{18} cm^{-3}, and as the cavity length of the laser increases, the threshold carrier density (i.e. total carrier density N in Fig. 6(a)) will decrease. This requires larger percentage of the carrier density of the HH1 first subband to form enough population inversion and realize laser emission because of this population mainly resulting from the HH1 first subband. This phenomenon agrees with variation
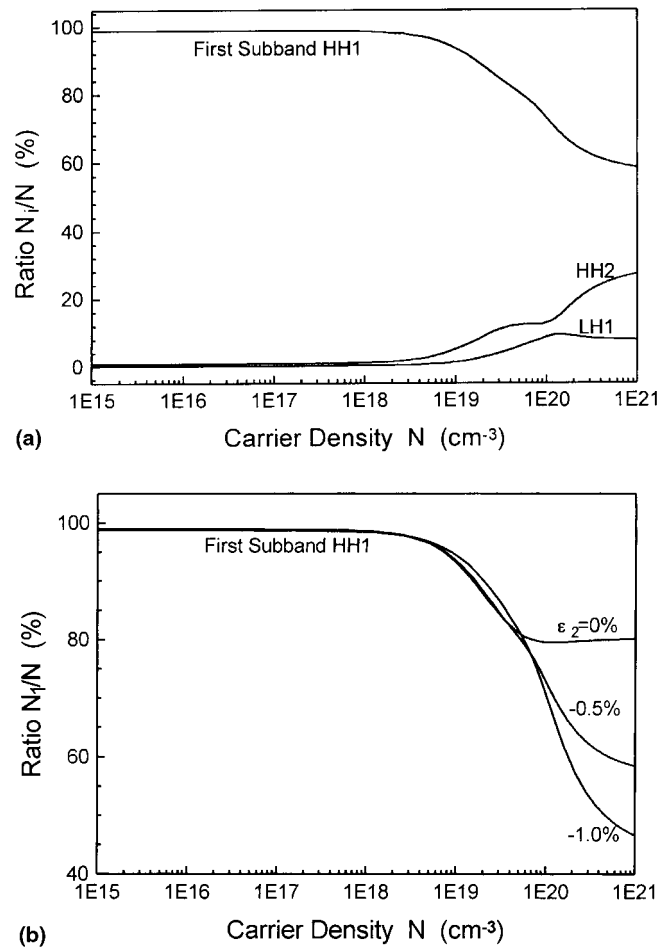

Fig. 6. Percentages of carrier density (a) N_i/N for HH1, HH2 and LH1 subbands and (b) N_1/N for HH1 first subband versus total carrier density N, where the well width $b_1 = 3.4$ nm, the barrier width $b_2 = 6.8$ nm, the compressive strain in the well $\varepsilon_1 = 1.5\%$, and the tensile strain in the barrier (a) $\varepsilon_2 = -0.5\%$, and (b) $\varepsilon_2 = 0$, -0.5 and -1.0%.

regularity of the percentage of the carrier density N_1/N of the HH1 first subband versus the total carrier density N as shown in Fig. 6(a). Fig 6(b) shows the effect of the tensile strain ε_2 in the barrier on the percentage of the carrier density N_1/N of HH1 first subband, where we take $\varepsilon_2 = 0$, -0.5 and -1.0%, respectively. We can find that the effect of the tensile strain ε_2 in the barrier on the percentage of the carrier density N_1/N of the HH1 first subband is very slight when the total carrier density N is less than 10^{18} cm^{-3}, while this effect is obvious when the total carrier density N is in the range of 10^{18}–10^{19} cm^{-3}. In this case, larger tensile strain in the barrier would cause larger percentage of the carrier density of the HH1 first subband, and hence results in larger threshold carrier density and higher threshold current density. Therefore, in order to reduce the threshold carrier density and threshold current density of the laser, the tensile strain in the barrier should not be selected too large.

5. Density of states in the valence band

5.1. DENSITY OF STATES IN DIFFERENT DIRECTIONS OF WAVEVECTOR $\vec{k}_\parallel$

Because the constant energy lines of the valence subbands are not circular, the density of states should have different values along different directions of the wavevector $\vec{k}_\parallel$ on a constant energy line, the expression of the density of states should be modified. By assuming θ being the angle between $\vec{k}_\parallel$ and k_x, the density of states of the ith valence subband along this direction can be written as

$$\rho_v^i(\theta) = \frac{2}{(2\pi)^2} k_\parallel \frac{\mathrm{d}k_\parallel}{\mathrm{d}E_i}, \tag{3}$$

so the density of states of all the valence subbands along this direction is given by

$$\rho_v(\theta) = \sum_i \rho_v^i(\theta) = \frac{2}{(2\pi)^2} \sum_i k_\parallel \frac{\mathrm{d}k_\parallel}{\mathrm{d}E_i} \cdot, \tag{4}$$

Fig. 7 plots the curves of the density of states $\rho_v(\theta)$ along different directions of the wavevector $\vec{k}_\parallel$ on some constant energy lines, where we take the tensile strain in the barrier as $\varepsilon_2 = 0$, -0.5 and -1.0%, and the energy values as $E_v = -50$, -100 and -150 mev, respectively. It can be seen that the curves of the density of states $\rho_v(\theta)$ are nearly straight near the top of the valence
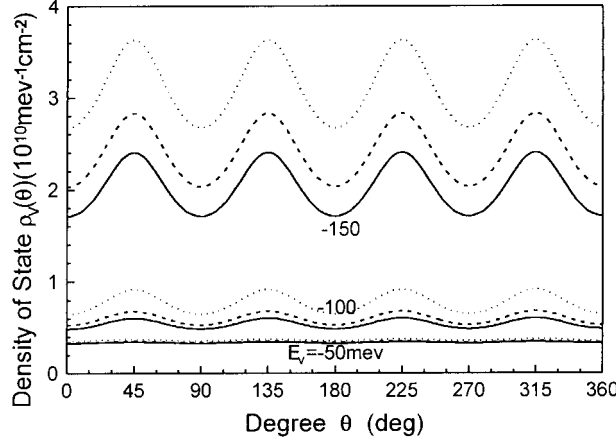
Fig. 7. Density of states $\rho_v(\theta)$ along different directions of wavevector $k_\parallel$, where the well width $b_1 = 3.4$ nm, the barrier width $b_2 = 6.8$ nm, the compressive strain in the well $\varepsilon_1 = 1.5\%$, the tensile strain in the barrier $\varepsilon_2 = 0\%$ (solid lines), -0.5% (dashed lines) and -1.0% (dotted lines), and the energy $E_v = -50, -100$ and -150 mev.

band. This indicates that the density of states $\rho_v(\theta)$ is nearly constant in different directions of the wavevector $\vec{k}_\parallel$ near the top of the valence band. When the energy is far from the top, however, the density of states $\rho_v(\theta)$ has different values along different directions of the wavevector $\vec{k}_\parallel$. It can also be found that the density of states $\rho_v(\theta)$ is a periodic function of the angle θ, of which the period is $\pi/2$.

5.2. TOTAL DENSITY OF STATES

The total density of states in all the valence subbands can be expressed as

$$\rho_v = \int_0^{2\pi} \rho_v(\theta)d\theta = \frac{2}{(2\pi)^2} \sum_i \int_0^{2\pi} k_\parallel \frac{dk_\parallel}{dE_i} d\theta. \qquad (5)$$

Fig. 8 shows the effect of the tensile strain ε_2 in the barrier on the total density of states ρ_v in the valence band, where we take the tensile strain in the barrier as $\varepsilon_2 = 0, -0.5$ and -1.0%, respectively. We can find that as the tensile strain ε_2 in the barrier increases, the total density of states ρ_v becomes larger. Therefore, the range of the strain compensation should be chosen properly. When the tensile strain in the barrier is within the range of $-0.5\% \leq \varepsilon_2 \leq 0\%$, the total density of states ρ_v varies slightly. So we can select some value of the barrier tensile strain ε_2 in this range to keep
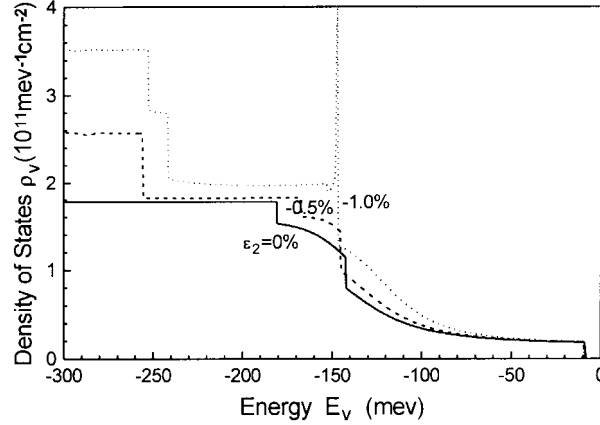
Fig. 8. Total density of states ρ_v versus valence band energy E_V, where the well width $b_1 = 3.4$ nm, the barrier width $b_2 = 6.8$ nm, the compressive strain in the well $\varepsilon_1 = 1.5\%$, and the tensile strain in the barrier $\varepsilon_2 = 0\%$ (solid lines), -0.5% (dashed lines) and -1.0% (dotted lines).

the total density of states smaller, for example, we can choose the tensile strain ε_2 in the barrier as -0.375% to form a zero net strain in the SCQW laser structure.

Similar calculations are also carried out for the cases of the compressive strain in the well as $\varepsilon_1 = 1.0$ and 2.0%, we have found that the larger the compressive strain in the well is, the lower the density of states becomes. So we can also select larger compressive strain in the well to reduce the density of states.

6. Optical gain

In terms of the formula presented in Derry *et al.* (1992), the optical gain g versus the wavelength λ, and the peak gain G versus the tensile strain ε_2 in the barrier are calculated for the TE polarization, and the results are shown in Figs. 9 and 10, respectively. In the calculation we take the carrier density as $N = 1.5\times$, $2.0\times$, $2.5\times$, and 3.0×10^{18} cm^{-3}, the temperature as $T = 300$ K, and the intraband relaxation time as $\tau_i = 0.1$ ps (Nido *et al.* 1993). It can be seen that as the tensile strain ε_2 in the barrier increases, the peak gain G decreases slightly, and its relative wavelength shifts from about 1.6 to 1.5 μm. This indicates that when the tensile strain in the barrier is within the range of $-0.5\% \leq \varepsilon_2 \leq 0\%$, the peak gain G drops a little, and the laser can be realized 1.55 μm wavelength emission.
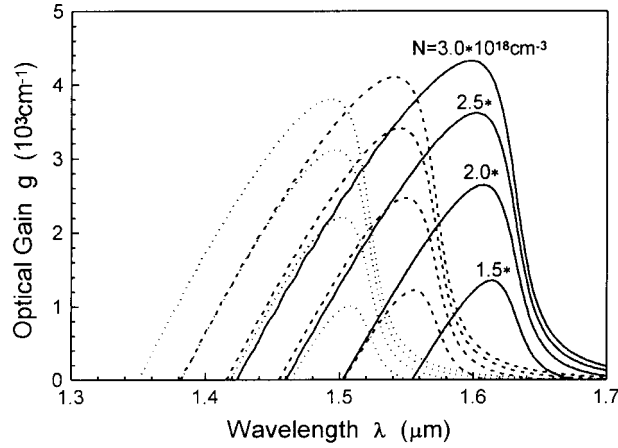
Fig. 9. Optical gain g versus wavelength λ for TE polarization, where the well width $b_1 = 3.4$ nm, the barrier width $b_2 = 6.8$ nm, the compressive strain in the well $\varepsilon_1 = 1.5\%$, the tensile strain in the barrier $\varepsilon_2 = 0\%$ (solid lines), -0.5% (dashed lines) and -1.0% (dotted lines), and the carrier density $N = 1.5\times$, $2.0\times$, $2.5\times$, and 3.0×10^{18} cm^{-3}.

7. Threshold property at zero net strain

The emission condition of the laser is given by

$$G_{\text{th}} = \frac{1}{\gamma b_1} \left(\alpha + \frac{1}{L} \ln \frac{1}{R} \right), \tag{6}$$

where G_{th} is the threshold gain, γ is the optical confinement fact of the unit width of the well, α is the loss coefficient, R is the facet reflectivity, and L is
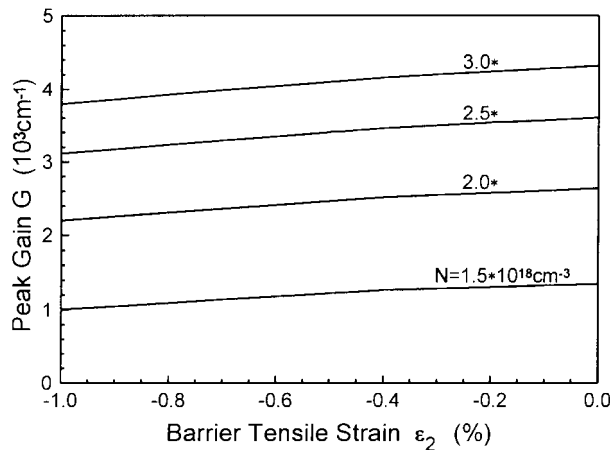

Fig. 10. Peak gain G versus tensile strain ε_2 in the barrier for TE polarization, where the well width $b_1 = 3.4$ nm, the barrier width $b_2 = 6.8$ nm, the compressive strain in the well $\varepsilon_1 = 1.5\%$, and the carrier density $N = 1.5\times$, $2.0\times$, $2.5\times$, and 3.0×10^{18} cm^{-3}.

the cavity length. In the calculation we take $\gamma = 1.8 \times 10^{-3}$ nm^{-1} (Lin and Lo 1993), $\alpha = 5.7$ cm^{-1} (Derry *et al.* 1992) and $R = 0.3$ (Derry *et al.* 1992). When the threshold gain G_{th} equals the peak gain G for some carrier density N, the laser becomes emission, the threshold wavelength $\lambda_{th} = \lambda|_{G=G_{th}}$, the threshold carrier density $N_{th} = N|_{G=G_{th}}$, and the threshold current density $J_{th} = J|_{G=G_{th}}$, where J is the injection current density, of which the expression is given in Derry *et al.* (1992), and the internal quantum efficiency is taken as $n = 0.85$ (Derry *et al.* 1992).

According to the principle of the net strain, the critical thickness should become infinite in theory when the net strain equals zero. In our laser configuration, that is, a 3.4 nm well with 1.5% compressive strain is inserted between two 6.8 nm barriers, in order to realize zero net strain in the structure, the tensile strain in the barrier should be selected as $\varepsilon_2 = -\varepsilon_1/4 = -0.375\%$. In this case, the total density of states is smaller and the peak gain is larger compared with the case of larger tensile strain in the barrier. In the meantime, the larger critical thickness is formed to avoid the occurrence of the defects in the material, this results in the improvement of the features of the SCQW lasers.

Fig. 11 shows the effect of the cavity length L on (a) the threshold wavelength λ_{th} and (b) the threshold carrier density N_{th} and the threshold current density J_{th} of a SCQW InGaAs/InGaAsP laser with a zero net strain, where the relative parameters chosen as: the well width $b_1 = 3.4$ nm, the barrier width $b_2 = 6.8$ nm, the compressive strain in the well $\varepsilon_1 = 1.5\%$, the tensile strain in the barrier $\varepsilon_2 = -0.375\%$. We can find that as the cavity length L decreases, the threshold wavelength λ_{th} decreases slightly, while the threshold carrier density N_{th} and the threshold current density J_{th} increases. We can also find that there is a limitation of the cavity length, that is, $L \approx 350$ μm, near which the threshold carrier density and the threshold current density become very large. Therefore, the cavity length had batter be taken larger than 400 μm for single SCQW lasers. When the cavity length L increases from 400 to 1000 μm, the threshold wavelength λ_{th} varies from about 1.54 to 1.56 μm, the threshold carrier density N_{th} varies from about 5.5 to 2.2×10^{18} cm^{-3}, and the threshold current density J_{th} varies from about 266 to 76.7 A cm^{-2}. When we select the cavity length $L = 520$ μm, the threshold wavelength λ_{th} is just 1.55 μm, and relative threshold carrier density N_{th} is 3.47×10^{18} cm^{-3} and threshold current density J_{th} is 150 A cm^{-2}.

8. Conclusion

On the basis of the above analysis and discussions for the InGaAs/InGaAsP SCQW lasers lattice-matched to InP substrate, some conclusions can be summarized.
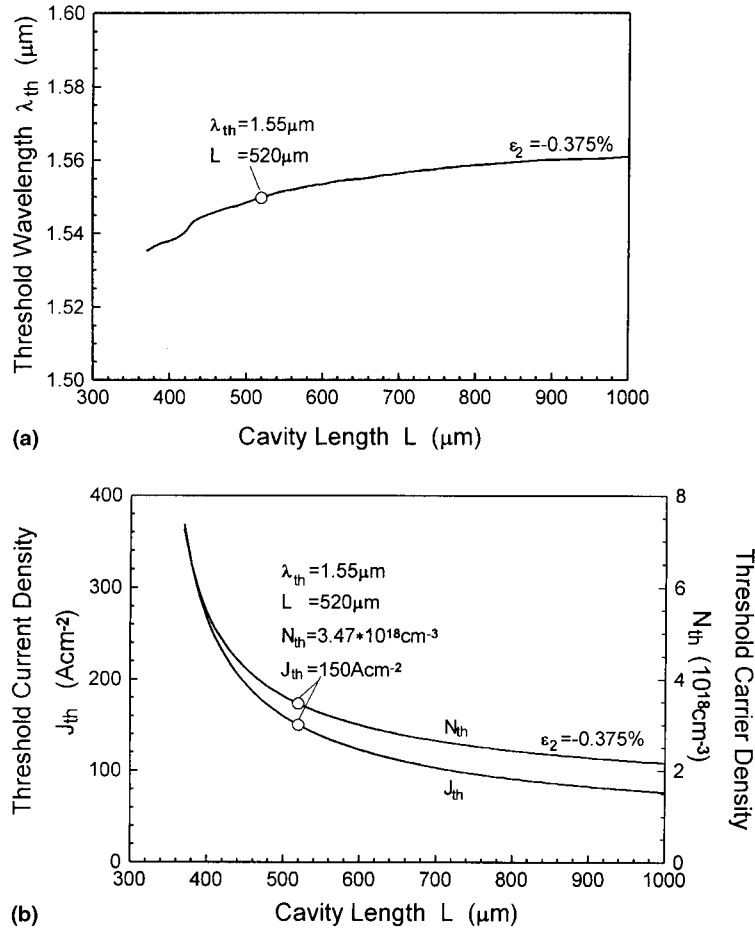
Fig. 11. (a) Threshold wavelength λ_{th}, and (b) threshold carrier density N_{th} and threshold current density J_{th} versus cavity length L at zero net strain, where the well width $b_1 = 3.4$ nm, the barrier width $b_2 = 6.8$ nm, the compressive strain in the well $\varepsilon_1 = 1.5\%$, and the tensile strain in the barrier $\varepsilon_2 = -0.375\%$.

In the usual case, typical 1.1 to 1.2 μm barrier bandgap is needed, which gives an enough range of strain compensation between the well and the barrier. The strain compensation affects the band offsets, so it should be limited properly to make the band offsets positive. Therefore, we had better select such a range of strain compensation that the strain in the well is compressive and that in the barrier is tensile to keep the SCQW system as type I.

Strain compensation changes the band structures and affects the features of the SCQW lasers. For a certain compressive strain in the well, the tensile strain in the barrier should be selected properly to obtain smaller density of states and higher peak gain. This can result in smaller threshold carrier density and lower threshold current density of the SCQW lasers.

We can choose zero net strain to increase the critical thickness and reduce the defects in the material. For the SCQW laser configuration adopted in this paper, that is, a 3.4 nm well with 1.5% compressive strain is inserted between two 6.8 nm barriers with −0.375% tensile strain, the net strain in the structure is zero. In addition, when we select the cavity length as 520 μm, the threshold wavelength is just 1.55 μm, and relative threshold carrier density is 3.47×10^{18} cm^{-3} and threshold current density is 150 A cm^{-2}.

Acknowledgment

References

Chua, C.L., C.H. Lin, Z.H. Zhu, Y.H. Lo, M. Hong, J.P. Mannaerts and R. Bhat. *IEEE Photon. Tec. Lett.* **6** 1400, 1994.

Derry, P.L., R.J. Fu, C.S. Hong, E.Y. Chan and L. Figueroa. *IEEE J. Quantum. Electron.* **28** 2698, 1992.

Hillmer, H., R. Lösch, F. Steinhagen, W. Schlapp, A. Pöcker and H. Burkhard. *Electron. Lett.* **31** 1346, 1995.

Hong, S.C., M. Jaffe and J. Singh. *IEEE J. Quantum. Electron.* **QE-23** 2181, 1987.

Ishikawa T. and J.E. Bowers. *IEEE J. Quantum. Electron.* **30** 562, 1994.

Kasukawa, A., N. Yokouchi, N. Yamanaka and N. Iwai. *Electron. Lett.* **31** 1749, 1995a.

Kasukawa, A., N. Yokouchi, N. Yamanaka, N. Iwai and T. Matsuda. *Jpn. J. Appl. Phys.* **34,** Pt. 2 L965, 1995b.

Lin, C.H., C.L. Chua, Z.H. Zhu, F.E. Ejeckam, T.C. Wu and Y.H. Lo. *Appl. Phys. Lett.* **64** 3395, 1994.

Lin C.H. and Y.H. Lo. *IEEE Photon. Tec. Lett.* **5** 288, 1993.

Ma, C.S., C.H. Han and S.Y. Liu. *Opt. Quantum Electron.* **29** 697, 1997.

Miller, B.I., U. Koren, M.G. Young and M.D. Chien. *Appl. Phys. Lett.* **58** 1952, 1991.

Nido, M., K. Naniwae, J. Shimizu, S. Murata and A. Suzuki. *IEEE J. Quantum. Elecctron.* **29** 885, 1993.

Ougazzaden, A., F. Devaux, E.V.K. Rao, L. Silvestre and G. Patriarche. *Appl. Phys. Lett.* **70** 96, 1997.

Ougazzaden, A., D. Sigogne, A. Mircea, E.V.K. Rao, A. Ramdane and L. Silvestre. *Electron. Lett.* **31** 1242, 1995.

Park, S.H., W.G. Jeong and B.D. Choe. *Appl. Phys. Lett.* **66** 201, 1995.

Silfvenious, C., B. Stalnacke and G. Landgren. *J. Crystal Growth* **170** 122, 1997.

Streubel, K., J. Wallin, G. Landgren, U. Öhlander, S. Lourdudoss and O. Kjebon. *J. Crystal Growth* **143** 7, 1976.

Tu, C.W., X.B. Mei, C.H. Yan and W.G. Bi. *Materials Sci. Eng.* B **35** 166, 1995.

Zhang G. and A. Ovtchinnikov, *Appl. Phys. Lett.* **62** 1644, 1993.